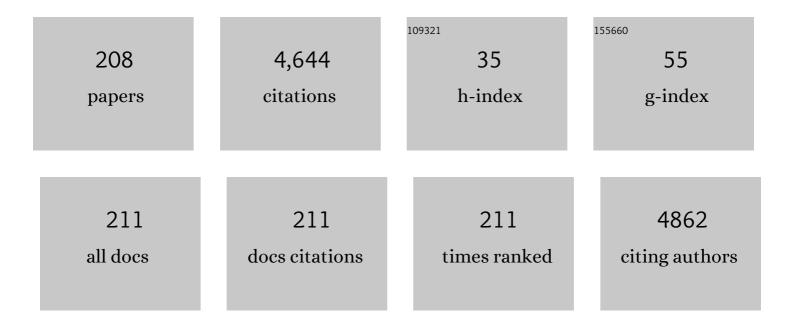
Maciej Sitarz

List of Publications by Year in descending order

Source: https://exaly.com/author-pdf/6385986/publications.pdf Version: 2024-02-01



#	Article	IF	CITATIONS
1	Infrared spectroscopy of different phosphates structures. Spectrochimica Acta - Part A: Molecular and Biomolecular Spectroscopy, 2011, 79, 722-727.	3.9	277
2	ldentification of silicooxygen rings in SiO2 based on IR spectra. Spectrochimica Acta - Part A: Molecular and Biomolecular Spectroscopy, 2000, 56, 1819-1823.	3.9	151
3	Structure of phosphate and iron-phosphate glasses by DFT calculations and FTIR/Raman spectroscopy. Journal of Non-Crystalline Solids, 2016, 450, 48-60.	3.1	129
4	Hierarchically structured lithium titanate for ultrafast charging in long-life high capacity batteries. Nature Communications, 2017, 8, 15636.	12.8	117
5	Spectroscopic studies of different aluminosilicate structures. Journal of Molecular Structure, 1999, 511-512, 251-257.	3.6	115
6	The structure of simple silicate glasses in the light of Middle Infrared spectroscopy studies. Journal of Non-Crystalline Solids, 2011, 357, 1603-1608.	3.1	114
7	Rings in the structure of silicate glasses. Journal of Molecular Structure, 1999, 511-512, 281-285.	3.6	108
8	Acid mine drainage (AMD) treatment: Neutralization and toxic elements removal with unmodified and modified limestone. Ecological Engineering, 2015, 81, 30-40.	3.6	99
9	Vibrational spectra of complex ring silicate anions — method of recognition. Journal of Molecular Structure, 1997, 404, 193-197.	3.6	87
10	Raman spectroscopy of TiO2 thin films formed by hybrid treatment for biomedical applications. Spectrochimica Acta - Part A: Molecular and Biomolecular Spectroscopy, 2014, 133, 867-871.	3.9	81
11	Synthesis, structural properties and thermal stability of Mn-doped hydroxyapatite. Journal of Molecular Structure, 2010, 976, 301-309.	3.6	77
12	Model of silicooxygen ring vibrations. Journal of Molecular Structure, 1998, 450, 229-238.	3.6	71
13	The effect of CaO/SiO 2 molar ratio of CaO-Al 2 O 3 -SiO 2 glasses on their structure and reactivity in alkali activated system. Spectrochimica Acta - Part A: Molecular and Biomolecular Spectroscopy, 2018, 194, 163-171.	3.9	68
14	The non-ring cations influence on silicooxygen ring vibrations. Journal of Molecular Structure, 2000, 555, 357-362.	3.6	67
15	Vibrational spectra of phosphate–silicate biomaterials. Journal of Molecular Structure, 2003, 651-653, 39-54.	3.6	64
16	Hydroxyapatite from animal bones – Extraction and properties. Ceramics International, 2015, 41, 4841-4846.	4.8	59
17	Vibrational spectra of aluminosilicate ring structures. Journal of Molecular Structure, 2002, 614, 273-279.	3.6	55
18	The effect of SiO2/Al2O3 ratio on the structure and microstructure of the glazes from SiO2–Al2O3–CaO–MgO–Na2O–K2O system. Spectrochimica Acta - Part A: Molecular and Biomolecula	ar3.9	55

Spectroscopy, 2015, 134, 621-630.

2

#	Article	IF	CITATIONS
19	Toward Highly Dispersed Mesoporous Bioactive Glass Nanoparticles With High Cu Concentration Using Cu/Ascorbic Acid Complex as Precursor. Frontiers in Chemistry, 2019, 7, 497.	3.6	55
20	Calculations of silicooxygen ring vibration frequencies. Spectrochimica Acta - Part A: Molecular and Biomolecular Spectroscopy, 1999, 55, 2831-2837.	3.9	51
21	Structure of multicomponent SiO2–Al2O3–Fe2O3–CaO–MgO glasses for the preparation of fibrous insulating materials. Journal of Molecular Structure, 2005, 744-747, 615-619.	3.6	50
22	Free carbon phase in SiOC glasses derived from ladder-like silsesquioxanes. Journal of Molecular Structure, 2016, 1126, 172-176.	3.6	50
23	Industrial products and wastes as adsorbents for sulphate and chloride removal from synthetic alkaline solution and mine process water. Chemical Engineering Journal, 2015, 259, 364-371.	12.7	48
24	Structural and luminescent properties of germanate glasses and double-clad optical fiber co-doped with Yb3+/Ho3+. Journal of Alloys and Compounds, 2017, 727, 1221-1226.	5.5	47
25	Oxidation, graphitization and thermal resistance of PCD materials with the various bonding phases of up to 800A°C. International Journal of Refractory Metals and Hard Materials, 2014, 45, 109-116.	3.8	44
26	Influence of zinc ions on structure, bioactivity, biocompatibility and antibacterial potential of melt-derived and gel-derived glasses from CaO-SiO2 system. Journal of Non-Crystalline Solids, 2019, 511, 86-99.	3.1	44
27	ICP, IR, Raman, NMR investigations of beryls from pegmatites of the Sudety Mts. Journal of Molecular Structure, 2005, 744-747, 1005-1015.	3.6	42
28	Spectroscopic studies of glassy phospho-silicate materials. Journal of Molecular Structure, 2005, 744-747, 621-626.	3.6	42
29	Effect of microwave treatment on structure of binders based on sodium carboxymethyl starch: FT-IR, FT-Raman and XRD investigations. Spectrochimica Acta - Part A: Molecular and Biomolecular Spectroscopy, 2018, 199, 387-393.	3.9	41
30	Structural studies of the NaCaPO4–SiO2 sol–gel derived materials. Journal of Molecular Structure, 2003, 651-653, 489-498.	3.6	39
31	Moraskoite, Na ₂ Mg(PO ₄)F, a new mineral from the Morasko IAB-MG iron meteorite (Poland). Mineralogical Magazine, 2015, 79, 387-398.	1.4	39
32	Spectroscopic study of biologically active glasses. Journal of Molecular Structure, 2005, 744-747, 609-614.	3.6	37
33	Influence of modifying cations on the structure and texture of silicate–phosphate glasses. Journal of Molecular Structure, 2008, 887, 237-248.	3.6	37
34	SiOC glasses produced from silsesquioxanes by the aerosol-assisted vapor synthesis method. Spectrochimica Acta - Part A: Molecular and Biomolecular Spectroscopy, 2013, 112, 440-445.	3.9	36
35	Spectroscopic characterization of Co3O4 catalyst doped with CeO2 and PdO for methane catalytic combustion. Spectrochimica Acta - Part A: Molecular and Biomolecular Spectroscopy, 2014, 131, 696-701.	3.9	36
36	FT-IR and FT-Raman studies of cross-linking processes with Ca2+ ions, glutaraldehyde and microwave radiation for polymer composition of poly(acrylic acid)/sodium salt of carboxymethyl starch – In moulding sands, Part II. Spectrochimica Acta - Part A: Molecular and Biomolecular Spectroscopy, 2015, 151, 27-33.	3.9	36

#	Article	IF	CITATIONS
37	Preparation of silver nanoparticles using different fractions of TEMPO-oxidized nanocellulose. European Polymer Journal, 2019, 116, 242-255.	5.4	35
38	FT-IR and FT-Raman studies of cross-linking processes with Ca2+ ions, glutaraldehyde and microwave radiation for polymer composition of poly(acrylic acid)/sodium salt of carboxymethyl starch – Part I. Spectrochimica Acta - Part A: Molecular and Biomolecular Spectroscopy, 2015, 135, 529-535.	3.9	34
39	Preparation and structural studies of black glasses based on ladder-like silsesquioxanes. Spectrochimica Acta - Part A: Molecular and Biomolecular Spectroscopy, 2014, 132, 884-888.	3.9	33
40	MORPHOLOGY, COMPOSITION AND STRUCTURE OF LOW-TEMPERATURE P4/nnc HIGH-FLUORINE VESUVIANITE WHISKERS FROM POLAR YAKUTIA, RUSSIA. Canadian Mineralogist, 2003, 41, 843-856.	1.0	32
41	Amorphous SiCxOy coatings from ladder-like polysilsesquioxanes. Journal of Molecular Structure, 2011, 993, 193-197.	3.6	31
42	The usefulness of walnut shells as waste biomass fuels in direct carbon solid oxide fuel cells. Biomass and Bioenergy, 2018, 119, 144-154.	5.7	31
43	Effect of GeO2 content on structural and spectroscopic properties of antimony glasses doped with Sm3+ ions. Journal of Molecular Structure, 2016, 1126, 207-212.	3.6	30
44	Bioactive layers based on black glasses on titanium substrates. Journal of the American Ceramic Society, 2018, 101, 590-601.	3.8	30
45	Removal of strontium (Sr 2+) from aqueous solutions with titanosilicates obtained by the sol–gel method. Journal of Colloid and Interface Science, 2015, 438, 159-168.	9.4	29
46	An Investigation into the Influence of Filler Silanization Conditions on Mechanical and Thermal Parameters of Epoxy Resin-Fly Ash Composites. Journal of Polymers and the Environment, 2016, 24, 298-308.	5.0	29
47	Cu SSZ-13 zeolite catalyst on metallic foam support for SCR of NO with ammonia: Catalyst layering and characterisation of active sites. Catalysis Today, 2016, 268, 142-149.	4.4	29
48	Hydroxyapatite/sodium alginate coatings electrophoretically deposited on titanium substrates: microstructure and properties. Applied Surface Science, 2021, 540, 148353.	6.1	29
49	Structural and optical study of tellurite–barium glasses. Journal of Molecular Structure, 2016, 1126, 219-225.	3.6	28
50	Fabrication and characterization of oxygen – Diffused titanium using spectroscopy method. Spectrochimica Acta - Part A: Molecular and Biomolecular Spectroscopy, 2014, 133, 883-886.	3.9	27
51	Structural and spectroscopic properties of lead phosphate glasses doubly doped with Tb 3+ and Eu 3+ ions. Journal of Molecular Structure, 2018, 1163, 418-427.	3.6	27
52	Spectroscopic studies of structural interactions in silicate-borate-phosphate glass. Journal of Molecular Structure, 2018, 1171, 110-116.	3.6	26
53	Cracking the Chloroquine Conundrum: The Application of Defective UiO-66 Metal–Organic Framework Materials to Prevent the Onset of Heart Defects—In Vivo and In Vitro. ACS Applied Materials & Interfaces, 2021, 13, 312-323.	8.0	26
54	Enhanced mid-infrared 2.7 μm luminescence in low hydroxide bismuth-germanate glass and optical fiber co-doped with Er3+/Yb3+ ions. Journal of Non-Crystalline Solids, 2017, 457, 169-174.	3.1	25

#	Article	IF	CITATIONS
55	Two-Step Procedure of Fly Ash Modification as an Alternative Method for Creation of Functional Composite. Journal of Polymers and the Environment, 2017, 25, 1342-1347.	5.0	25
56	Structural and microstructural comparison of bioactive melt-derived and gel-derived glasses from CaO-SiO2 binary system. Ceramics International, 2018, 44, 8856-8863.	4.8	25
57	Metal Foams as Novel Catalyst Support in Environmental Processes. Catalysts, 2019, 9, 587.	3.5	25
58	Si-DEFICIENT, OH-SUBSTITUTED, BORON-BEARING VESUVIANITE FROM THE WILUY RIVER, YAKUTIA, RUSSIA. Canadian Mineralogist, 2003, 41, 833-842.	1.0	24
59	Micro-Raman spectroscopy studies of some accessory minerals from pegmatites of the Sowie Mts and Strzegom-SobA³tka massif, Lower Silesia, Poland. Journal of Molecular Structure, 2005, 744-747, 1017-1026.	3.6	24
60	Structure and microstructure of glasses from a NaCaPO4–SiO2–BPO4 system. Vibrational Spectroscopy, 2012, 61, 72-77.	2.2	24
61	Analysis of thermal and structural properties of germanate glasses co-doped with Yb3+/Tb3+ ions. Spectrochimica Acta - Part A: Molecular and Biomolecular Spectroscopy, 2014, 131, 702-707.	3.9	24
62	Structural and optical study on antimony-silicate glasses doped with thulium ions. Spectrochimica Acta - Part A: Molecular and Biomolecular Spectroscopy, 2015, 134, 608-613.	3.9	24
63	New high temperature amorphous protective coatings for Mg2Si thermoelectric material. Ceramics International, 2019, 45, 10230-10235.	4.8	24
64	Effect of structural properties of carbon-based fuels on efficiency of direct carbon fuel cells. Journal of Solid State Electrochemistry, 2014, 18, 3023-3032.	2.5	23
65	Influence of Ar-irradiation on structural and nanomechanical properties of pure zirconium measured by means of GIXRD and nanoindentation techniques. Journal of Molecular Structure, 2016, 1126, 226-231.	3.6	23
66	The formation of the Co 3 O 4 cobalt oxide within CoO substrate. Corrosion Science, 2016, 112, 536-541.	6.6	23
67	Electrophoretic deposition and microstructure development of Si3N4/polyetheretherketone coatings on titanium alloy. Surface and Coatings Technology, 2018, 350, 633-647.	4.8	23
68	In Search of Effective UiO-66 Metal–Organic Frameworks for Artificial Kidney Application. ACS Applied Materials & Interfaces, 2021, 13, 45149-45160.	8.0	23
69	Structural role of Fe in the soil active glasses. Spectrochimica Acta - Part A: Molecular and Biomolecular Spectroscopy, 2011, 79, 728-732.	3.9	22
70	Thermal evolution of ladder-like silsesquioxanes during formation of black glasses. Journal of Thermal Analysis and Calorimetry, 2017, 130, 103-111.	3.6	20
71	Spectroscopic studies of electrophoretically deposited hybrid HAp/CNT coatings on titanium. Spectrochimica Acta - Part A: Molecular and Biomolecular Spectroscopy, 2014, 133, 872-875.	3.9	19
72	Impact of ZnO on the structure of aluminosilicate glazes. Journal of Molecular Structure, 2016, 1126, 251-258.	3.6	19

#	Article	IF	CITATIONS
73	Microstructure study of opaque glazes from SiO2–Al2O3–MgO–K2O–Na2O system by variable molar ratio of SiO2/Al2O3 by FTIR and Raman spectroscopy. Journal of Molecular Structure, 2016, 1126, 240-250.	3.6	19
74	Non-Noble Metal Oxide Catalysts for Methane Catalytic Combustion: Sonochemical Synthesis and Characterisation. Nanomaterials, 2017, 7, 174.	4.1	19
75	Functional properties of poly(tetrafluoroethylene) (PTFE) gasket working in nuclear reactor conditions. Journal of Molecular Structure, 2018, 1157, 306-311.	3.6	19
76	Crystallization of silico-phosphate glasses. Journal of Thermal Analysis and Calorimetry, 2008, 91, 255-260.	3.6	18
77	Natural and synthetic hydroxyapatite/zirconia composites: A comparative study. Ceramics International, 2016, 42, 11126-11135.	4.8	18
78	Cytotoxicity, chemical stability, and surface properties of ferroelectric ceramics for biomaterials. Journal of the American Ceramic Society, 2018, 101, 440-449.	3.8	18
79	Influence of the replacement of silica by boron trioxide on the properties of bioactive glass scaffolds. International Journal of Applied Glass Science, 2021, 12, 293-312.	2.0	18
80	Moganite in selected Polish chert samples: The evidence from MIR, Raman and X-ray studies. Spectrochimica Acta - Part A: Molecular and Biomolecular Spectroscopy, 2014, 122, 55-58.	3.9	17
81	Structural characterization and evaluation of antibacterial and angiogenic potential of gallium-containing melt-derived and gel-derived glasses from CaO-SiO2 system. Ceramics International, 2018, 44, 22698-22709.	4.8	17
82	Crystallization study of sol–gel derived 13-93 bioactive glass powder. Journal of the European Ceramic Society, 2021, 41, 1695-1706.	5.7	17
83	Chemical and spectroscopic characterization of some phosphate accessory minerals from pegmatites of the Sowie GA³ry Mts, SW Poland. Journal of Molecular Structure, 2009, 924-926, 442-447.	3.6	16
84	The structure and bonding properties of chosen phenyl ladder-like silsesquioxane clusters. Journal of Molecular Structure, 2013, 1044, 314-322.	3.6	16
85	Importance of the electronic structure of modified TiO 2 in the photoelectrochemical processes of hydrogen generation. International Journal of Hydrogen Energy, 2015, 40, 815-824.	7.1	16
86	The impact of physicochemical properties of coal on direct carbon solid oxide fuel cells. International Journal of Hydrogen Energy, 2016, 41, 18872-18883.	7.1	16
87	Shift in low-frequency vibrational spectra measured in-situ at 600°C by Raman spectroscopy of zirconia developed on pure zirconium and Zr–1%Nb alloy. Journal of Molecular Structure, 2016, 1126, 186-191.	3.6	16
88	Optimization of Ti/Ta2O5–SnO2 electrodes and reaction parameters for electrocatalytic oxidation of methylene blue. Journal of Applied Electrochemistry, 2016, 46, 349-358.	2.9	16
89	Characterisation of well-adhered ZrO2 layers produced on structured reactors using the sonochemical sol–gel method. Applied Surface Science, 2018, 427, 563-574.	6.1	16
90	Rare earth-doped barium gallo-germanate glasses and their near-infrared luminescence properties. Spectrochimica Acta - Part A: Molecular and Biomolecular Spectroscopy, 2018, 201, 362-366.	3.9	16

#	Article	IF	CITATIONS
91	A Sustainable Autoclaved Material Made of Glass Sand. Buildings, 2019, 9, 232.	3.1	16
92	Voids in mixed-cation silicate glasses: Studies by positron annihilation lifetime and Fourier transform infrared spectroscopies. Spectrochimica Acta - Part A: Molecular and Biomolecular Spectroscopy, 2014, 129, 643-648.	3.9	15
93	Structural and microstructural studies of zinc-doped glasses from NaCaPO4-SiO2 system. Journal of Non-Crystalline Solids, 2016, 441, 66-73.	3.1	15
94	An investigation of the effect of silicone oil on polymer intraocular lenses by means of PALS, FT-IR and Raman spectroscopies. Spectrochimica Acta - Part A: Molecular and Biomolecular Spectroscopy, 2016, 167, 96-100.	3.9	15
95	DeNOx Abatement over Sonically Prepared Iron-Substituted Y, USY and MFI Zeolite Catalysts in Lean Exhaust Gas Conditions. Nanomaterials, 2018, 8, 21.	4.1	15
96	Luminescent Studies on Germanate Glasses Doped with Europium Ions for Photonic Applications. Materials, 2020, 13, 2817.	2.9	15
97	Influence of modifiers and glass-forming ions on the crystallization of glasses of the NaCaPO4–SiO2 system. Journal of Thermal Analysis and Calorimetry, 2012, 109, 577-584.	3.6	14
98	In situ and operando spectroscopic studies of sonically aided catalysts for biogas exhaust abatement. Journal of Molecular Structure, 2016, 1126, 132-140.	3.6	14
99	Thermal characterisation of raw aluminosilicate glazes in SiO2–Al2O3–CaO–K2O–Na2O–ZnO system with variable content of ZnO. Journal of Thermal Analysis and Calorimetry, 2017, 128, 1343-1351.	3.6	14
100	Si-O-C amorphous coatings for high temperature protection of In0.4Co4Sb12 skutterudite for thermoelectric applications. Journal of Applied Physics, 2019, 125, 215113.	2.5	14
101	Studying functional properties of hydrogel and silicone–hydrogel contact lenses with PALS, MIR and Raman spectroscopy. Spectrochimica Acta - Part A: Molecular and Biomolecular Spectroscopy, 2014, 131, 686-690.	3.9	13
102	Structure and thermal properties of the fritted glazes in SiO2–Al2O3–CaO–MgO–Na2O–K2O–ZnO system. Journal of Thermal Analysis and Calorimetry, 2017, 130, 165-176.	3.6	13
103	From Nanoparticle Assembly to Monolithic Aerogels of YAG, Rare Earth Fluorides, and Composites. Chemistry of Materials, 2018, 30, 5460-5467.	6.7	13
104	In-situ XRD investigations of FeAl intermetallic phase-based alloy oxidation. Corrosion Science, 2020, 164, 108344.	6.6	13
105	Modification of SiOC-based layers with cerium ions - influence on the structure, microstructure and corrosion resistance. Applied Surface Science, 2021, 543, 148871.	6.1	13
106	Chemical and Structural Characterization of Amorphous and Crystalline Alumina Obtained by Alternative Sol–Gel Preparation Routes. Materials, 2021, 14, 1761.	2.9	13
107	FTIR studies of the cyclosilicate-like structures. Journal of Molecular Structure, 2001, 596, 185-189.	3.6	12
108	Aluminium influence on the crystallization and bioactivity of silico-phosphate glasses from NaCaPO4–SiO2 system. Journal of Non-Crystalline Solids, 2010, 356, 224-231.	3.1	12

#	Article	IF	CITATIONS
109	Direct crystallization of silicate–phosphate glasses of NaCaPO4–SiO2 system. Journal of Thermal Analysis and Calorimetry, 2013, 113, 1363-1368.	3.6	12
110	Thermal resistance of PCD materials with borides bonding phase. Journal of Superhard Materials, 2015, 37, 155-165.	1.2	12
111	Structural and optical properties of antimony-germanate-borate glass and glass fiber co-doped Eu3+ and Ag nanoparticles. Spectrochimica Acta - Part A: Molecular and Biomolecular Spectroscopy, 2018, 201, 1-7.	3.9	12
112	Design and Application of High Optical Quality YAG:Ce Nanocrystal-Loaded Silica Aerogels. ACS Applied Materials & Interfaces, 2018, 10, 32304-32312.	8.0	12
113	Effect of the Processing and Heat Treatment Route on the Microstructure of MoS2/Polyetheretherketone Coatings Obtained by Electrophoretic Deposition. Journal of the Electrochemical Society, 2019, 166, D151-D161.	2.9	12
114	Effect of Low-Friction Composite Polymer Coatings Fabricated by Electrophoretic Deposition and Heat Treatment on the Ti-6Al-4V Titanium Alloy's Tribological Properties. Metallurgical and Materials Transactions A: Physical Metallurgy and Materials Science, 2020, 51, 4786-4798.	2.2	12
115	Organobentonites Modified with Poly(Acrylic Acid) and Its Sodium Salt for Foundry Applications. Materials, 2021, 14, 1947.	2.9	12
116	Development of Geopolymers Based on Fly Ashes from Different Combustion Processes. Polymers, 2022, 14, 1954.	4.5	12
117	The aluminium effect on the structure of silico-phosphate glasses studied by NMR and FTIR. Journal of Molecular Structure, 2009, 924-926, 107-110.	3.6	11
118	Vibrational spectra of a baghdadite synthetic analogue. Vibrational Spectroscopy, 2015, 76, 1-5.	2.2	11
119	Spectroscopic properties of transparent Er-doped oxyfluoride glass–ceramics with GdF3. Spectrochimica Acta - Part A: Molecular and Biomolecular Spectroscopy, 2015, 134, 631-637.	3.9	11
120	Raman and FTIR spectra of nephrites from the ZÅ,oty Stok and Jordanów ÅšlÄski (the Sudetes and) Tj ETQqO	0 0 rgBT / 3.6	Overlock 10 T
121	Holmium doped barium gallo-germanate glasses for near-infrared luminescence at 2000â€ ⁻ nm. Journal of Luminescence, 2019, 215, 116625.	3.1	11
122	Influence of transition metal ion concentration on near-infrared emission of Ho3+ in barium gallo-germanate glasses. Journal of Alloys and Compounds, 2019, 793, 107-114.	5.5	11
123	The structure of liquation silico-phosphate glasses. Journal of Molecular Structure, 2008, 887, 229-236.	3.6	10
124	From nanometric zirconia powder to transparent polycrystal. Journal of the European Ceramic Society, 2014, 34, 4321-4326.	5.7	10
125	Influence of aluminium and boron ions on the crystallization of silicate–phosphate glasses from the NaCaPO4â^'SiO2 system. Journal of Non-Crystalline Solids, 2014, 401, 207-212.	3.1	10
126	Stress analysis of zirconia studied by Raman spectroscopy at low temperatures. Spectrochimica Acta -	3.9	10

Part A: Molecular and Biomolecular Spectroscopy, 2014, 131, 691-695. 126

#	Article	IF	CITATIONS
127	Pore structure and sorption characterization of titanosilicates obtained from concentrated precursors by the sol–gel method. RSC Advances, 2015, 5, 72562-72571.	3.6	10
128	Effect of hybrid oxidation on the titanium oxide layer's properties investigated by spectroscopic methods. Journal of Molecular Structure, 2016, 1126, 165-171.	3.6	10
129	Structural and thermal studies of modified silica-strontium-barium glass from CRT. Journal of Molecular Structure, 2016, 1126, 265-274.	3.6	10
130	Analysis of upconversion luminescence in germanate glass and optical fiber codoped with Yb^3+/Tb^3+. Applied Optics, 2016, 55, 2370.	2.1	10
131	Key Properties of a Bioactive Ag-SiO2/TiO2 Coating on NiTi Shape Memory Alloy as Necessary at the Development of a New Class of Biomedical Materials. International Journal of Molecular Sciences, 2021, 22, 507.	4.1	10
132	Electrochemical characterization of anti-corrosion coatings formed on 6061 aluminum alloy by plasma electrolytic oxidation in the corrosion inhibitor-enriched aqueous solutions. Electrochimica Acta, 2022, 424, 140652.	5.2	10
133	FT-IR studies of cyclogermanates. Vibrational Spectroscopy, 2002, 29, 45-51.	2.2	9
134	Optical Characterization of Nano- and Microcrystals of EuPO4 Created by One-Step Synthesis of Antimony-Germanate-Silicate Glass Modified by P2O5. Materials, 2017, 10, 1059.	2.9	9
135	Structural studies of tellurite glasses doped with erbium ions. Journal of Molecular Structure, 2018, 1164, 328-333.	3.6	9
136	The structure of model glasses of the amorphous phase of glass-ceramic glazes from the SiO2Al2O3CaO MgO Na2O K2O ZnO system. Journal of Non-Crystalline Solids, 2019, 515, 125-132.	3.1	9
137	Production of vitrified material from hazardous asbestos-cement waste and CRT glass cullet. Journal of Cleaner Production, 2021, 317, 128345.	9.3	9
138	Polymer Derived Ceramics based on SiAlOC glasses as novel protective coatings for ferritic steel. Applied Surface Science, 2022, 576, 151826.	6.1	9
139	Single-crystal Raman investigation of vesuvianite in the OH region. Vibrational Spectroscopy, 2007, 44, 36-41.	2.2	8
140	Theoretical and experimental spectroscopic studies of Bi dopant location in Mg2Si. Vibrational Spectroscopy, 2015, 76, 31-37.	2.2	8
141	Optical and vibrational properties of phosphorylcholine-based contact lenses—Experimental and theoretical investigations. Spectrochimica Acta - Part A: Molecular and Biomolecular Spectroscopy, 2017, 176, 83-90.	3.9	8
142	Structural studies of tellurite glasses from the 70TeO2-5XO-10P2O5–10ZnO–5PbF2 system (XÂ= Ba, W,) Tj	ETQq00	0 rgBT /Overl
143	Experimental and Theoretical Studies of Sonically Prepared Cu–Y, Cu–USY and Cu–ZSM-5 Catalysts for SCR deNOx. Catalysts, 2021, 11, 824.	3.5	8

144	The aluminium effect on the phospho-silicate materials. Journal of Molecular Structure, 2002, 614, 289-295.	3.6	7
	209 2951		

#	Article	IF	CITATIONS
145	Influence of iron contaminations on local and bulk magnetic properties of nonfunctionalized and functionalized multiâ€wall carbon nanotubes. Physica Status Solidi (A) Applications and Materials Science, 2014, 211, 661-669.	1.8	7
146	Ammonolysis of gallium phosphide GaP to the nanocrystalline wide bandgap semiconductor gallium nitride GaN. RSC Advances, 2015, 5, 106128-106140.	3.6	7
147	Structure and microstructure of the glasses from NaCaPO4–SiO2 and NaCaPO4–SiO2–AlPO4 systems. Journal of Molecular Structure, 2016, 1126, 47-62.	3.6	7
148	Low-temperature synthesis of silicon carbide powder using shungite. Boletin De La Sociedad Espanola De Ceramica Y Vidrio, 2017, 56, 39-46.	1.9	7
149	Cold Plasma Synthesis and Testing of NiOX-Based Thin-Film Catalysts for CO2 Methanation. Catalysts, 2021, 11, 905.	3.5	7
150	Effect of Y2O3 additive on morphology and phase composition of zirconia solid solutions. Ceramics International, 2022, 48, 13055-13062.	4.8	7
151	The effect of inversion of matrix and inclusions composition in liquation phospho-silicate glasses. Spectrochimica Acta - Part A: Molecular and Biomolecular Spectroscopy, 2011, 79, 739-742.	3.9	6
152	Thermal annealing effect on physical properties of DNA–CTMA thin films. Optical Materials, 2013, 36, 36-41.	3.6	6
153	Nanoscale Observation of Dehydration Process in PHEMA Hydrogel Structure. Nanoscale Research Letters, 2017, 12, 303.	5.7	6
154	Investigation of the influence of pretreatment parameters on the surface characteristics of amorphous metal for use in power industry. Journal of Molecular Structure, 2018, 1160, 360-367.	3.6	6
155	Parafiniukite, Ca2Mn3(PO4)3Cl, a New Member of the Apatite Supergroup from the Szklary Pegmatite, Lower Silesia, Poland: Description and Crystal Structure. Minerals (Basel, Switzerland), 2018, 8, 485.	2.0	6
156	Effect of ZrO 2 sol-gel coating on the Ti 99.2 – Porcelain bond strength investigated with mechanical testing and Raman spectroscopy. Journal of Molecular Structure, 2018, 1168, 316-321.	3.6	6
157	Synthesis of boron carbide powders from mono- and polysaccharides. International Journal of Refractory Metals and Hard Materials, 2020, 86, 105099.	3.8	6
158	Influence of GLAD Sputtering Configuration on the Crystal Structure, Morphology, and Gas-Sensing Properties of the WO3 Films. Coatings, 2020, 10, 1030.	2.6	6
159	The crystallization and structure features of glass within the K2O–MgO–CaO–Al2O3–SiO2-(BaO) system. Journal of Molecular Structure, 2020, 1220, 128747.	3.6	6
160	Samples of Ba1â^'xSrxCe0.9Y0.1O3â^'Î′, 0 < x < 0.1, with Improved Chemical Stability in CO2-H2 Gas-Involving Atmospheres as Potential Electrolytes for a Proton Ceramic Fuel Cell. Materials, 2020, 13, 1874.	2.9	6
161	Amorphous Silicon Oxynitride-Based Powders Produced by Spray Pyrolysis from Liquid Organosilicon Compounds. Materials, 2021, 14, 386.	2.9	6
162	The Utilisation of Solid Fuels Derived from Waste Pistachio Shells in Direct Carbon Solid Oxide Fuel Cells. Materials, 2021, 14, 6755.	2.9	6

#	Article	IF	CITATIONS
163	Influence of Cr Ion Implantation on Physical Properties of CuO Thin Films. International Journal of Molecular Sciences, 2022, 23, 4541.	4.1	6
164	Spectroscopic Characterization of Silicate Amorphous Materials. Challenges and Advances in Computational Chemistry and Physics, 2019, , 457-481.	0.6	5
165	Hydroxyapatite of natural origin - zirconia composites, preparation and reactions within the system. Processing and Application of Ceramics, 2016, 10, 219-225.	0.8	5
166	Microstructure and Selected Properties of Advanced Biomedical n-HA/ZnS/Sulfonated PEEK Coatings Fabricated on Zirconium Alloy by Duplex Treatment. International Journal of Molecular Sciences, 2022, 23, 3244.	4.1	5
167	Generation of carbon nanostructures with diverse morphologies by the catalytic aerosol-assisted vapor-phase synthesis method. Comptes Rendus Chimie, 2015, 18, 1198-1204.	0.5	4
168	Vibrational spectroscopic characterization of the magnesium borate-phosphate mineral lüneburgite. Spectroscopy Letters, 2016, 49, 606-612.	1.0	4
169	Adsorption of caesium (Cs+) from aqueous solution by porous titanosilicate xerogels. Desalination and Water Treatment, 2016, 57, 5554-5566.	1.0	4
170	Functionalization of Ti99.2 substrates surface by hybrid treatment investigated with spectroscopic methods. Journal of Molecular Structure, 2018, 1164, 412-419.	3.6	4
171	Influence of SrO content on microstructure and crystallization of glazes in the SiO2–Al2O3–CaO–MgO–K2O system. Journal of Thermal Analysis and Calorimetry, 2019, 138, 4177-418	36. ^{3.6}	4
172	Impact of the synthesis parameters on the microstructure of nano-structured LTO prepared by glycothermal routes and 7Li NMR structural investigations. Journal of Sol-Gel Science and Technology, 2019, 89, 225-233.	2.4	4
173	Enhancing CO2 Conversion to CO over Plasma-Deposited Composites Based on Mixed Co and Fe Oxides. Catalysts, 2021, 11, 883.	3.5	4
174	New Ceramics Precursors Containing Si and Ge Atoms—Cubic Germasilsesquioxanes—Synthesis, Thermal Decomposition and Spectroscopic Analysis. Molecules, 2022, 27, 1441.	3.8	4
175	Corrosion Resistance and Electrical Conductivity of Hybrid Coatings Obtained from Polysiloxane and Carbon Nanotubes by Electrophoretic Co-Deposition. International Journal of Molecular Sciences, 2022, 23, 2897.	4.1	4
176	Paper material containing Ag cations immobilised in faujasite: synthesis, characterisation and antibacterial effects. Cellulose, 2018, 25, 1353-1364.	4.9	3
177	Spectroscopic studies of the silicone oil impact on the ophthalmic hydrogel based materials conducted in time dependent mode. Spectrochimica Acta - Part A: Molecular and Biomolecular Spectroscopy, 2018, 192, 1-5.	3.9	3
178	Raman spectroscopic studies of O–H stretching vibration in Mn-rich apatites: A structural approach. American Mineralogist, 2020, 105, 1385-1391.	1.9	3
179	Structural Characterization of Fine γ′-Fe4N Nitrides Formed by Active Screen Plasma Nitriding. Metals, 2020, 10, 1656.	2.3	3
180	Surface Properties and Morphology of Boron Carbide Nanopowders Obtained by Lyophilization of Saccharide Precursors. Materials, 2021, 14, 3419.	2.9	3

#	Article	IF	CITATIONS
181	2.7 μm emission in heavy metal oxide glasses doped with erbium ions. Proceedings of SPIE, 2015, , .	0.8	2
182	Spectroscopic characterization of rare hydrated ammonium borate mineral larderellite. Journal of Molecular Structure, 2018, 1159, 226-232.	3.6	2
183	Green up-conversion luminescence of erbium-doped oxyfluoride germanate fiber under continuous-wave laser-diode excitation. Materials Letters, 2018, 216, 131-134.	2.6	2
184	Application of TPO/TPR methods in oxidation investigations of CoSb3 and Mg2Si thermoelectrics with and without a protective coating of "black glass― Journal of Thermal Analysis and Calorimetry, 2020, 140, 2657-2666.	3.6	2
185	Dehydroxylation of Perlite and Vermiculite: Impact on Improving the Knock-Out Properties of Moulding and Core Sand with an Inorganic Binder. Materials, 2021, 14, 2946.	2.9	2
186	Application of Statistical Methods in Predicting the Properties of Glass-Ceramic Materials Obtained from Inorganic Solid Waste. Materials, 2021, 14, 2651.	2.9	2
187	Investigation of Dye Dopant Influence on Electrooptical and Morphology Properties of Polymeric Acceptor Matrix Dedicated for Ternary Organic Solar Cells. Polymers, 2021, 13, 4099.	4.5	2
188	Biochemical changes of macrophages and U87MG cells occurring as a result of the exposure to iron oxide nanoparticles detected with the Raman microspectroscopy. Spectrochimica Acta - Part A: Molecular and Biomolecular Spectroscopy, 2022, 278, 121337.	3.9	2
189	Near-infrared emission and energy transfer in tellurite glasses co-doped with erbium and thulium ions. Proceedings of SPIE, 2014, , .	0.8	1
190	Spectroscopic properties of the Pr3+ ion in TeO2-WO3-PbO-La2O3 and TeO2-WO3-PbO-Lu2O3 glasses. Open Physics, 2014, 12, .	1.7	1
191	Near infrared luminescence in Yb3+/Ho3+: co-doped germanate glass. , 2015, , .		1
192	Mid-infrared luminescence in HMO glass co-doped with Ho3+/Yb3+ ions. , 2016, , .		1
193	1.5 – 2.1 μm Broadband ASE in Rare-Earth Co-Doped Glasses and Double-Clad Optical Fibers. , 2018, , .		1
194	Chemical Structure and Microstructure Characterization of Ladder-Like Silsesquioxanes Derived Porous Silicon Oxycarbide Materials. Materials, 2021, 14, 1340.	2.9	1
195	PALS, MIR and UV–vis–NIR spectroscopy studies of pHEMA hydrogel, silicon- and fluoro-containing contact lens materials. Journal of Molecular Structure, 2017, 1148, 521-530.	3.6	1
196	Silver and copper modified zeolite imidazole frameworks as sustainable methane storage systems. Journal of Cleaner Production, 2022, 352, 131638.	9.3	1
197	Design of structured reactor for biogas exhaust abatement. Chemical Engineering Journal, 2022, 446, 136940.	12.7	1
198	Thermal, structural and spectroscopic properties of heavy metal oxide glass and glass-ceramics doped with Er3+ions. , 2015, , .		0

#	Article	IF	CITATIONS
199	Investigation of luminescent properties of LaF3:Nd3+nanoparticles. , 2015, , .		0
200	Investigation on Bioactivity of Zirconium-Calcium Coatings on Titanium Surface Obtained by Sol-Gel and Electrophoretic Deposition (EPD) Methods. Key Engineering Materials, 0, 687, 65-70.	0.4	0
201	Comparative analysis of luminescent properties of germanate glass and double-clad optical fibers co-doped with Yb ³⁺ /Ho ³⁺ ions. Proceedings of SPIE, 2016, , .	0.8	0
202	Upconversion luminescence in bismuth-germanate oxide glasses co-doped with lanthanide ions. Proceedings of SPIE, 2017, , .	0.8	0
203	Luminescent properties of germanium-based glasses and optical fiber co-doped with rare earth. Proceedings of SPIE, 2017, , .	0.8	0
204	Effect of Ag content on structural and luminescent properties of antimony-germanate-silicate glass doped with Eu3+ ions. , 2017, , .		0
205	Reply to the comment to: Bioactive layers based on black glasses on titanium substrates. Journal of the American Ceramic Society, 2018, 101, 3245-3245.	3.8	0
206	Spectroscopic properties and energy transfer in Er/Ag co-doped antimony oxide glass. , 2017, , .		0
207	Spectroscopic properties of rare earth doped germanate glasses. , 2018, , .		0
208	Spectroscopic and rheological investigation of candidates for the double-layered binder for amorphous metal ribbon. Journal of Molecular Structure, 2020, 1207, 127763.	3.6	0